DP-MS-76-65

CONF-770312--3

FRACTOGRAPHY OF HYDROGEN-EMBRITTLED STAINLESS STEEL*

G. R. Caskey, Jr.

Savannah River Laboratory
E. I. du Pont de Nemours and Company
Aiken, South Carolina 29801

Paper for Presentation at the
106th AIME Annual Meeting
Atlanta, Georgia
March 6-10, 1977

---

* This paper was prepared in connection with work under Contract No. AT(07-2)-1 with the U. S. Energy Research and Development Administration.

DISCLAIMER

FRACTOGRAPHY OF HYDROGEN-EMBRITTLED STAINLESS STEEL*

G. R. Caskey, Jr.
Savannah River Laboratory
E. I. du Pont de Nemours and Company
Aiken, South Carolina 29801

INTRODUCTION

Ductility of many austenitic stainless steels is reduced by charging with hydrogen or by testing in a hydrogen atmosphere.[1,2] Embrittlement is substantial with ductility losses of up to 50% when Type 304L stainless steel is tested in 69-MPa hydrogen.[1] Other varieties of stainless steel, such as Type 310, are affected only slightly under the same conditions, but embrittlement can be induced by cathodic charging where very high hydrogen contents can be attained.[3,4] The relatively high susceptibility of Type 304L stainless steel to hydrogen embrittlement has been attributed to the strain-induced transformation to α'-martensite[5,6] and more recently to coplanar dislocation motion.[1,7]

Changes in the morphology of the fracture have been observed in tensile specimens tested in hydrogen. Void formation and coalescence

---

* The information contained in this article was developed during the course of work under Contract No. AT(07-2)-1 with the U. S. Energy Research and Development Administration.

leading to a dimpled fracture is the only fracture mode observed in hydrogen-free Type 304L stainless steel. In contrast, features referred to as regular striations,[2] quasicleavage,[5] intergranular fracture,[5] and facets[6] have been reported for hydrogen-embrittled Type 304L. In addition, specimens deformed in high-pressure hydrogen have extensive surface cracking.[1] The cracks form at low strains and are associated with the surface layer deformed during machining.[1]

The present investigation was initiated to explore the temperature dependence of embrittlement of Type 304L stainless steel saturated with hydrogen at high pressure. This charging condition was expected to accentuate property changes and changes in fracture mode reported previously without the complicating effects associated with cathodic charging.[3] A clearer description of the embrittlement process and a possible change in fracture mode were anticipated. The present discussion emphasizes the initial fractographic and metallographic examination of the specimens. Further work is in progress.

SPECIMEN PREPARATION

Smooth bar tensile specimens of 0.48-cm diameter and 3.5-cm gauge length were machined from annealed bar stock of Type 304L stainless steel. Four of eight specimens were charged by exposure to deuterium at 69-MPa pressure for 1449 days at 473 K. All eight specimens were pulled in tension on an Instron testing machine (Instron Corporation, Canton, MA) at a cross-head speed

of 0.05 cm/minute. Pairs of specimens (one free of deuterium and the other charged) were pulled to fracture at temperatures of 380, 273, 198, and 78 K. Mechanical properties of the specimens are summarized in Table I. Saturation with deuterium increased the yield strength of the austenite at all test temperatures and embrittled the specimens at the two intermediate test temperatures.

Deuterium content of the specimens was measured by a vacuum-extraction technique. Samples were cut from the ends of the tensile specimens and placed in a small stainless steel container attached to a Consolidated Electrodynamics Corporation Type 24-120B leak detector. The specimens were heated to 750 K, and the deuterium offgassing rate was continuously monitored. Deuterium content was determined from the area under the offgassing curve and specimen weight. The average deuterium concentration of the four specimens was $\sim$200 mol/m^3 (4.4 cm^3 D_2/cm^3 alloy), which is less than anticipated for the exposure conditions based on published solubility data for austenitic stainless steel.[8]

Fracture surfaces were examined on a scanning electron microscope. In addition, the specimens were inspected at low magnification. Longitudinal sections through the gauge portion and transverse sections through the ends of the specimens were prepared for optical metallography. An oxalic acid electroetch was used to develop the microstructure.

FRACTOGRAPHY

Four features observed on the fracture faces of the tensile specimens are: facets, dimples, striations, and secondary cracks (Figure 1). Dimpled rupture was the only fracture mode observed on the deuterium-free specimens. The other three fracture modes were found only on the two specimens that were saturated with deuterium and tested at the two intermediate temperatures. The deuterium-saturated specimens tested at 78 and 380 K were not embrittled, and the only fracture mode was dimpled rupture.

Facets

The dominant feature on the fracture surfaces of the two embrittled specimens is the presence of facets (Figure 1). These highly reflective, flat areas were not confined to any particular part of the surface but were distributed uniformly (Figure 2) and are more numerous on the specimen fractured at 198 K than on the one broken at 273 K. In addition, steps and diagonal traces are observed on the facets (Figure 3). The steps are usually shallow, irregular in outline, and do not extend beyond the particular facet where they are located. Inclusions that intersect facets lack the characteristic dimple associated with them in regions of ductile rupture.

In all cases, three sets of diagonal traces appear on the facets. Each set is composed of roughly parallel markings that appear to delineate intersection of the facet surface with microstructural features below the surface. Frequently, one set of

traces will be more predominant than the others (Figure 4). Angles between pairs of traces are consistent with the hypothesis that all of the traces, as well as the plane of the facet, are {111} planes in the parent austenite. The traces, therefore, could arise from twins in the austenite, α'-martensite, or ε-martensite because the habit planes for all three of these microstructural features are {111} planes in the austenite. Facet shape, steps, and trace angles suggest that the facets have formed along twins in the austenite, which are always present in annealed Type 304L austenitic stainless steel. The traces then would arise from intersection of a facet face with strain-induced transformation to ε- and α'-martensite. The alternative explanation, that the facets are grain faces, appears less likely given the regularity of the traces that are always observed on the facets and the apparent constancy of the angles between traces.

Additional support for identification of the facets as annealing twin boundaries is obtained from inspection of longitudinal sections through the broken specimens. Many cracks are observed in the embrittled specimens, diminishing in frequency as the distance from the fracture face is increased. These cracks are often along twin boundaries (Figure 5), in which case, the cracks are straight and relatively flat.

Dimpled Rupture

Dimpled rupture is the only fracture mode in common among all of the specimens. In the deuterium-free specimens, the ridges between the dimples appear more pronounced in the central region than in the shear lips (Figure 6). In both areas, dimple sizes have a distinct bimodal distribution. The same characteristics were observed in the specimens that had been saturated with deuterium (Figure 7). In this case, however, dimple sizes appear somewhat smaller than in the deuterium-free specimens.

Striations

Both specimens that were embrittled by the deuterium had areas (Figure 8) designated as striations. They appear over more or less flat areas intermixed among facets and small areas of dimpled rupture (Figure 3). In each area, the dominant dimension of the striations is uniformly oriented. Their appearance is somewhat more distinct at 198 than at 273 K.

Secondary Cracks

Small cracks roughly parallel to the tensile axis were observed on the deuterium-saturated specimens tested at 198 and 273 K. The faces of these cracks are relatively smooth, but fine dimples can be seen in some cases (Figure 9).

Surface Cracks

Surface cracks on the deuterium-saturated specimen tested at 273 K (Figure 10) are identical in appearance to those formed on specimens of Type 304L stainless steel pulled to failure in a high-pressure hydrogen atmosphere. The cracks extend to a maximum depth of about 0.01 cm in the deuterium-saturated specimen. Although ductility loss was greater at 198 than at 273 K, only a few surface cracks were on surfaces of specimens tested at the lower temperature. The faces of some surface cracks were examined in detail. Striations were common, but occasionally facets were observed with them (Figure 4).

Discussion

The facets observed on the fractured surfaces of Type 304L stainless steel embrittled by saturation with hydrogen lay on or parallel to annealing twins in the austenite. The twinning plane in austenite is any one of the {111} planes. Slip planes and the habit plane for ε-martensite are {111} planes also. Consequently, during plastic deformation, slip may proceed on planes parallel to the twin in the parent crystal and on planes intersecting it in the twin depending upon the orientation of the twin planes with respect to the tensile axis. Similarly, ε-martensite may parallel or intersect the coherent twin boundary. Possible dislocation interactions that may arise from these processes are: dislocation pileups at incoherent boundaries along the twin or grain boundaries at the ends of the twin, formation of Lomar or Cottrell-Lomar locks

at the coherent twin boundary, annihilation of dislocations at the twin boundary, and cross-slip if the coherent twin boundary contains the slip direction. If hydrogen transport and concentration by dislocation motion is accepted as a necessary part of a mechanism for hydrogen embrittlement, one or more of these interactions may provide the specific dislocation mechanism for crack initiation and propagation. A detailed evaluation of the interactions has not been completed; however, the appearance of the facets suggests that dislocation pileups at incoherent twin boundaries may be the critical process.

Embrittlement of the specimens was greater and facets were more frequent at 198 than at 273 K. The number of annealing twins per unit volume is determined during recrystallization or annealing and should be the same in both specimens; therefore, the embrittlement is related to details of the deformation process at the two temperatures. The quantity of hydrogen transported per unit length of dislocation is greater at the lower temperature, assuming a dislocation-hydrogen interaction energy of $\sim 10^{-8}$ joule. In addition, the volume fraction of ε-martensite per unit deformation is greater at the lower temperature[9] because of a decrease in stacking fault energy with decreasing temperature.[10] Both of these factors would contribute to decreasing ductility by raising the hydrogen concentration to a critical level with less overall plastic deformation.

Observations of surface cracks have been reported for Type 304L stainless steel and *Tenelon** pulled to failure in high pressure hydrogen at room temperature.[1] The present study shows that this phenomenon is not restricted to environmental hydrogen embrittlement but may also arise in internal hydrogen embrittlement. Furthermore, surface cracking appears to be confined to a narrower temperature range than internal embrittlement and does not correlate with internal embrittlement. The most severe surface cracking was observed at 273 K; whereas, the most severe embrittlement was observed at 198 K where surface cracking was almost absent.

Secondary cracks and striations are characteristic of embrittled specimens also. Their origins are not evident but may be associated with mechanisms similar to those that cause facet formation.

CONCLUSIONS

Embrittlement of Type 304L stainless steel saturated with hydrogen at high pressure is characterized by reduction in uniform elongation, loss of necking strain, and appearance of facets on the fracture face. Ductility loss is greater at 198 than at 273 K, and there is essentially no ductility loss at 78 or 380 K. Surface cracks are profuse at 273 K but occur only occasionally at 198 K.

Facets on the fracture face of the embrittled specimens are believed to form along twin boundaries in the austenite. Several

---

* Trademark of United States Steel Corporation for 18% Cr, 15% Mn, 0.5% N, balance Fe.

dislocation mechanisms are possible to account for the facets and loss of tensile ductility. Further evaluation is needed to develop these mechanisms and to establish which if any may be critical to hydrogen embrittlement.

If the suggested role of annealing twins is borne out by subsequent analysis, stacking fault energy takes on added significance. Not only does a low stacking fault energy contribute to hydrogen embrittlement by increasing coplanar slip and concentration of hydrogen, but also a low stacking fault energy increases the frequency of annealing twins. Together these effects can provide the barriers to dislocation movement and the means to accumulate hydrogen at the barrier.

REFERENCES

1. M. R. Louthan, Jr. "Effects of Hydrogen on the Mechanical Properties of Low Carbon and Austenitic Steels." p. 53 in *Hydrogen in Metals*. I. M. Bernstein and A. W. Thompson (Editors), ASM, Metals Park, OH (1974).

2. M. R. Louthan, Jr., G. R. Caskey, Jr., J. A. Donovan, and D. E. Rawl, Jr. "Hydrogen Embrittlement of Metals." *Mater. Sci. Eng. 10*, 357 (1972).

3. M. L. Holzworth. "Hydrogen Embrittlement of Type 304L Stainless Steel. *Corrosion 25*, No. 3, 107 (1969).

4. J. Burke, A. Jeckels, P. Maulik, and M. L. Mebta. "The Effect of Hydrogen on the Structure and Properties of Fe-Ni-Cr Austenite." p. 102 in *Effect of Hydrogen on Behavior of Materials*. A. W. Thompson and I. M. Bernstein (Editors), AIME, New York (1976).

5. R. M. Vennett and G. S. Ansell. "The Effect of High-Pressure Hydrogen upon the Tensile Properties and Fracture Behavior of 304L Stainless Steel." *Trans. ASM 60*, 242 (1967).

6. R. B. Benson, Jr., R. K. Dann, and L. W. Roberts, Jr. "Hydrogen Embrittlement of Stainless Steel." *Trans. Met. Soc. AIME 242*, 2199 (1968).

7. J. K. Tien, A. W. Thompson, I. M. Bernstein, and Rebecca J. Richards. "Hydrogen Transport by Dislocations." *Met. Trans. 7A*, 821 (1976).

8. M. R. Louthan, Jr., and R. G. Derrick. "Hydrogen Transport in Austenitic Stainless Steel." *Corrosion Science 15*, 565 (1975).

9. C. J. Guntner and R. P. Reed. "The Effect of Experimental Variables Including the Martensitic Transformation on the Low-Temperature Mechanical Properties of Austenitic Stainless Steels." *Trans. ASM 55*, 399, (1962).

10. F. Lecroisey and A. Pineau. "Martensitic Transformations Induced by Plastic Deformation in the Fe-Ni-Cr-C System." *Met. Trans. 3*, 387 (1972).

TABLE I

Temperature Dependence of Hydrogen Embrittlement of Type 304L Austenitic Stainless Steel

Test Temp, K	*Deuterium Content, mol/m³*	*Strength, MPa*		*Elongation, %*		*Reduction in Area, %*
		Yield[a]	*Ultimate*[b]	*Uniform*	*Total*	
380	0	240	680	58	69	83
	200	260	730	60	70	72
273	0	310	1160	80	89	79
	190	330	870	44	44	36
198	0	360	1500	61	70	72
	190	390	1210	44	44	22
78	0	390	2200	60	64	72
	210	430	2100	59	65	72

---

a. Stress at $\varepsilon_p = 0.05$.

b. True stress at maximum load.

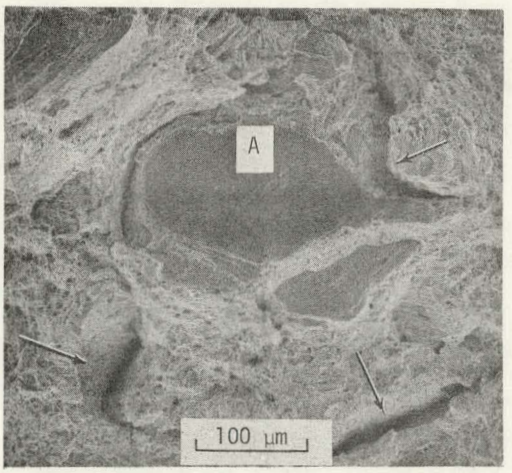

Facet A and Secondary Cracks (arrow)

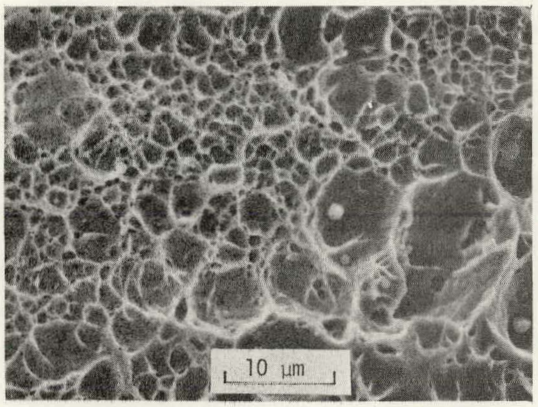

Dimple

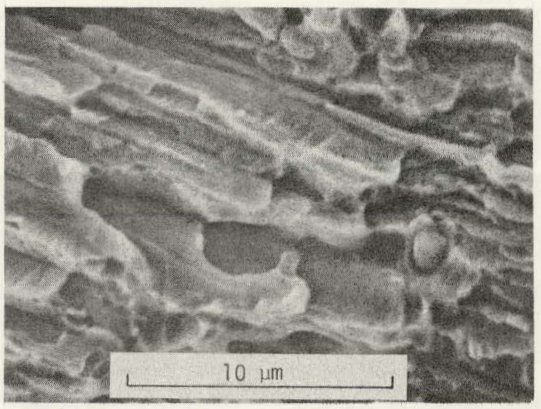

Striation

FIGURE 1. Fracture Surfaces of Type 304L Stainless Steel

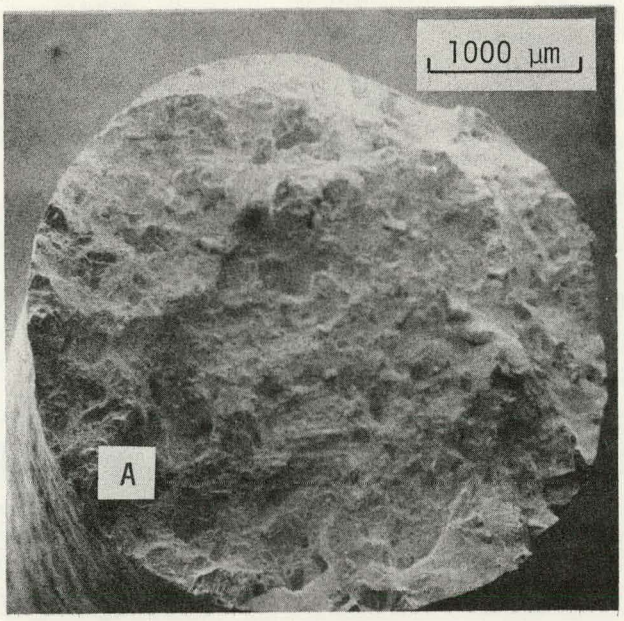

Facet Distribution Over Fracture Face

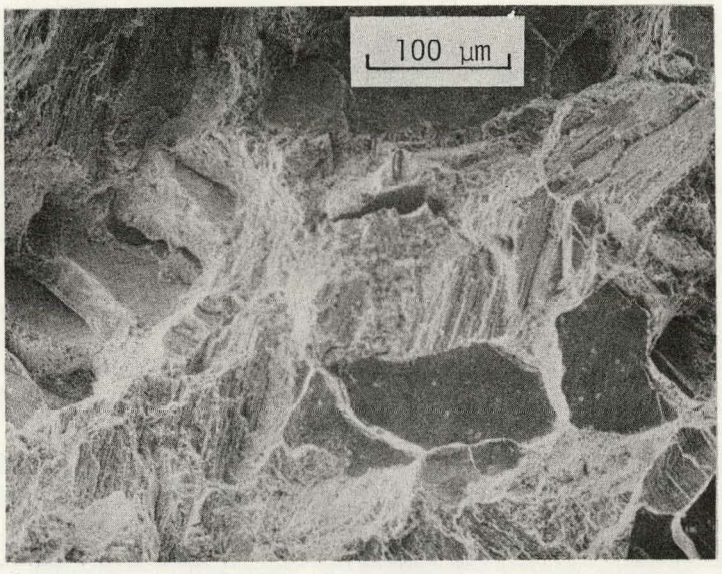

Detail at A

FIGURE 2. Facets on Deuterium-Saturated Specimen Tested at 198 K

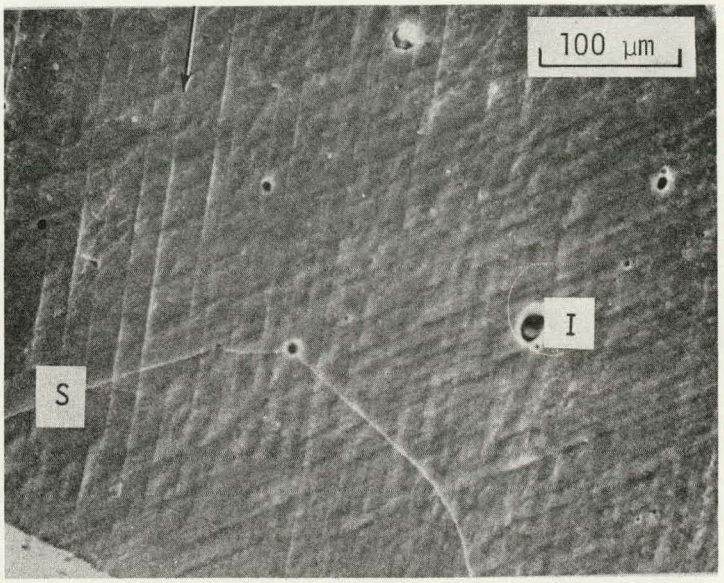

FIGURE 3. Facet Showing Step (S), Inclusion (I), and Trace (arrow) on Specimen Tested at 198 K

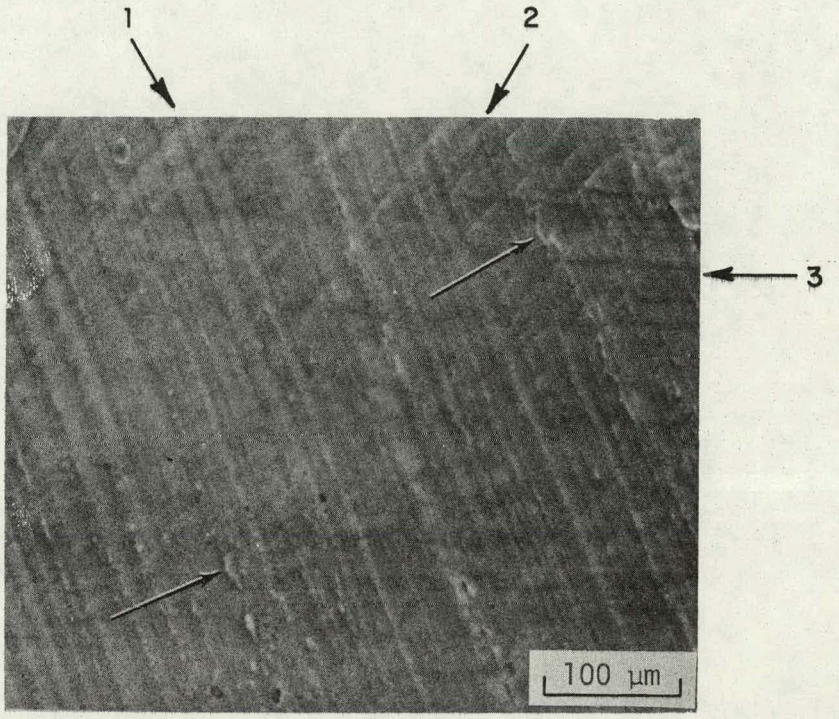

FIGURE 4. Facet Showing Three Sets of Traces [Note irregularities (arrow) along edge of dominant set.]

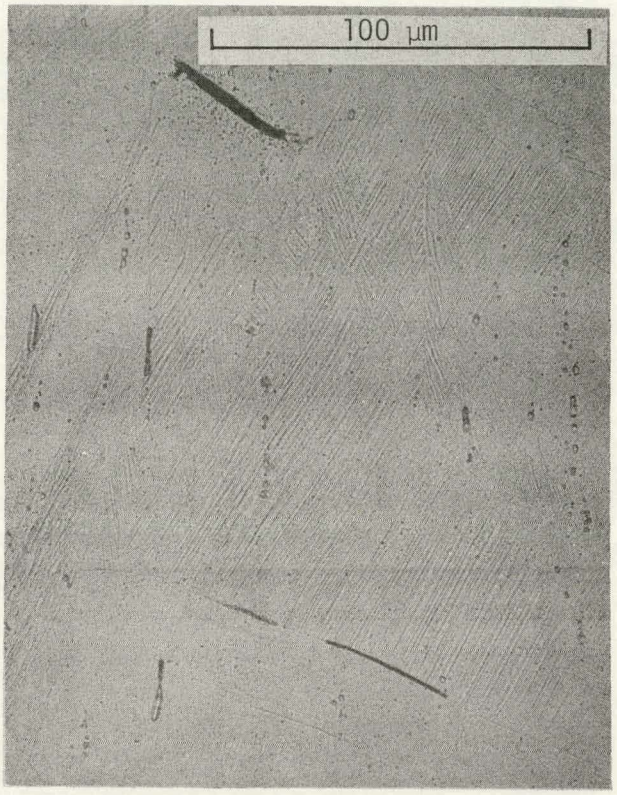

FIGURE 5. Longitudinal Section Showing Cracks Along Twin Boundaries at Test Temperature of 198 K

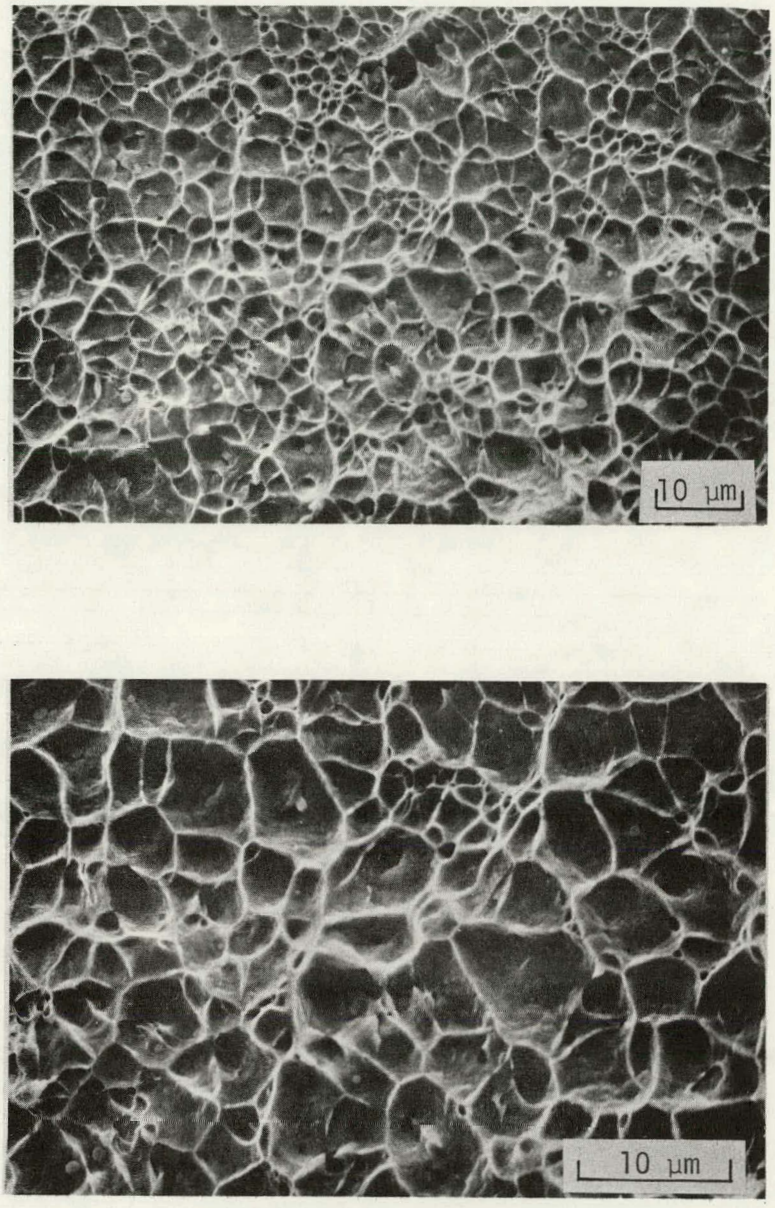

FIGURE 6. Dimpled Rupture of Deuterium-Free Specimen Tested at 273 K

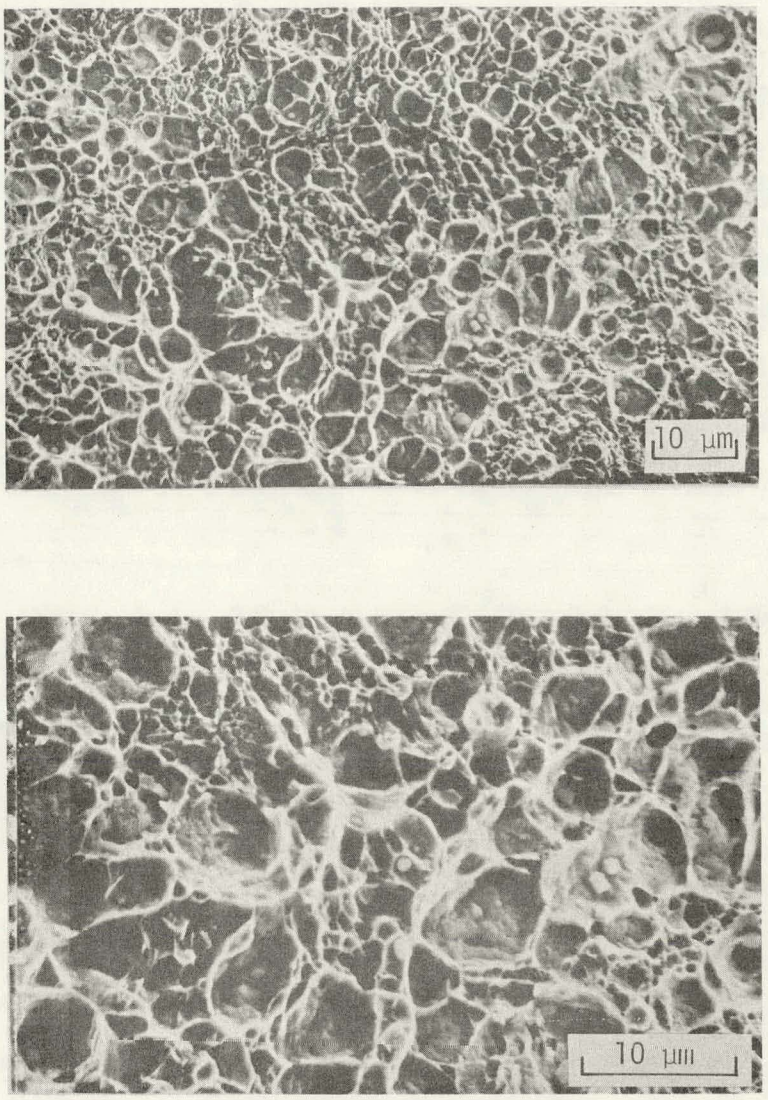

FIGURE 7. Dimpled Rupture of Deuterium-Saturated Specimen Tested at 273 K

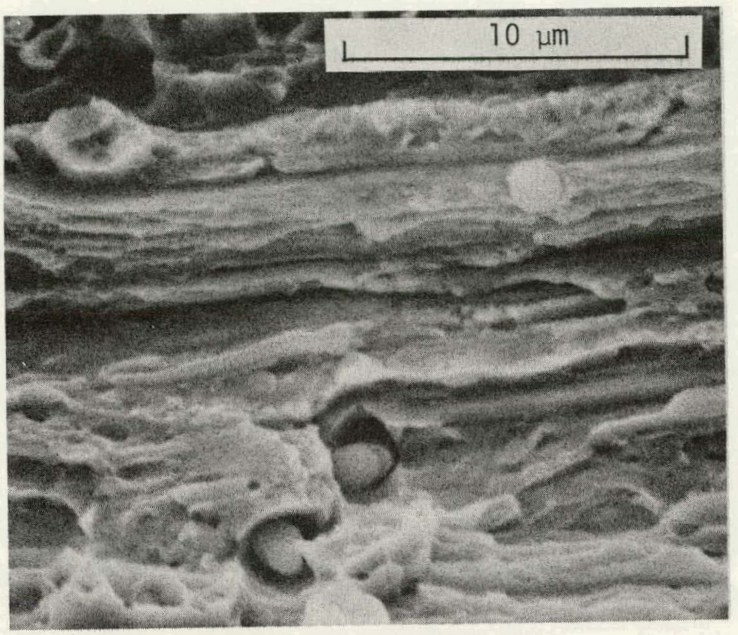

FIGURE 8. Striations Near Center of Deuterium-Saturated Specimen Tested at 273 K

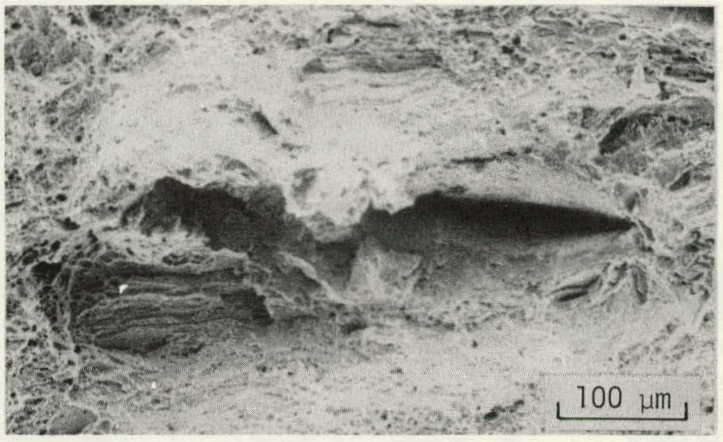

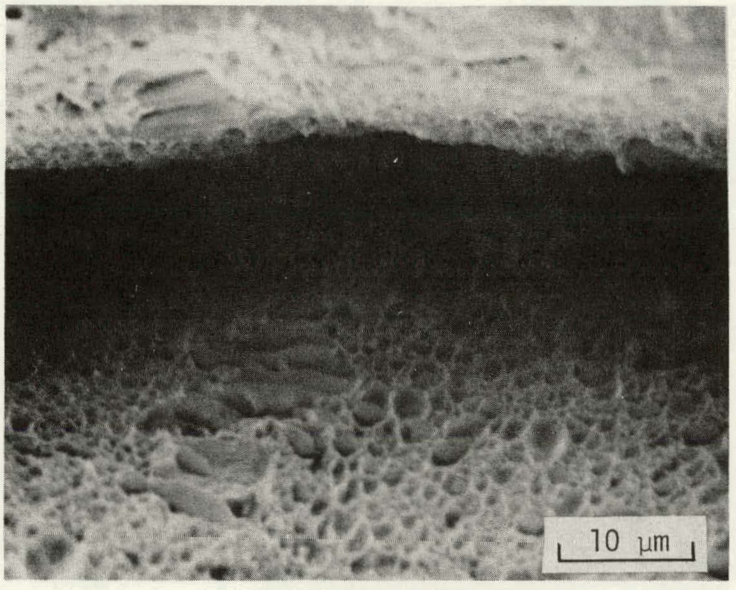

FIGURE 9. Secondary Crack With Dimpled Surface of Deuterium-Saturated Specimen Tested at 273 K

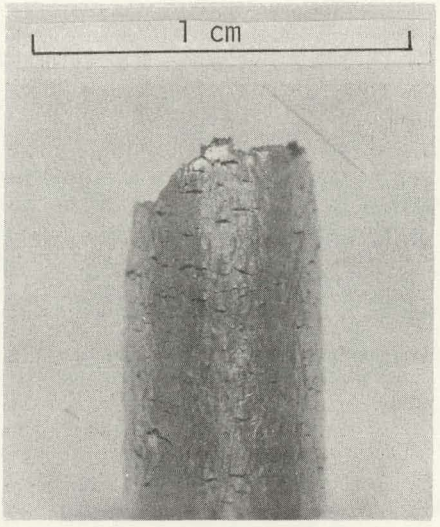

FIGURE 10. Surface Cracks of Deuterium-Saturated Specimen Tested at 273 K

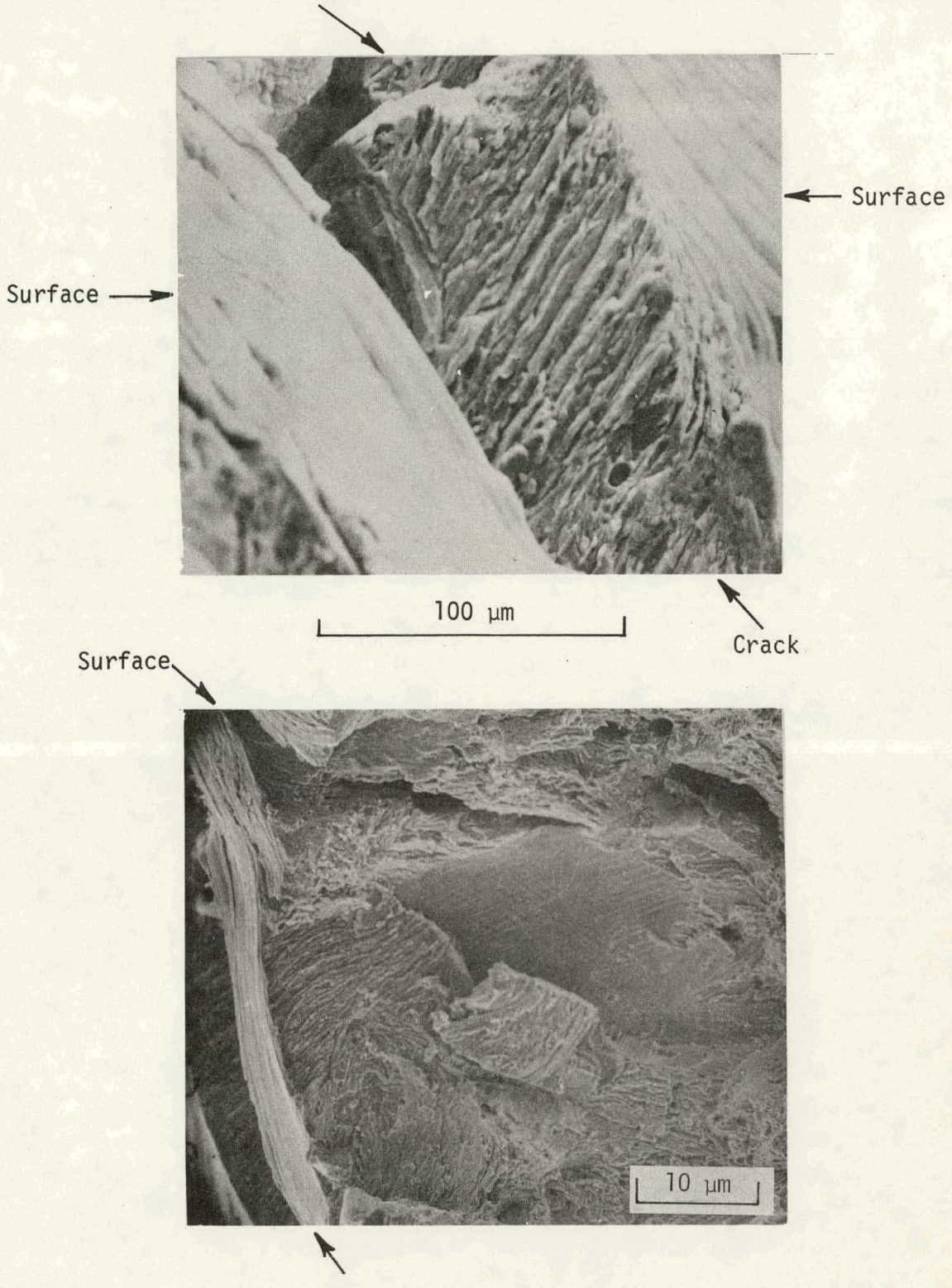

FIGURE 10. (Continued)